INVESTIGATION ON THE UNSTEADY AERODYNAMICS OF AN INDUSTRIAL FAN

Domenico BORELLO [1], Alessandro CORSINI [1], Franco RISPOLI [1], Anthony G. SHEARD[2]

[1] *University of Rome - Sapienza, Department of Mechanical and Aerospace Engineering, Via Eudossiana, 18, 00184 Roma, Italy*

[2] *Fläkt Woods Ltd, Axial Way, CO4 5ZG Colchester, Essex, United Kingdom*

SUMMARY

There are controversial requirements involved in developing numerical methodologies in order to compute the flow in industrial fans. The full resolution of turbulence spectrum in such high Reynolds number flow configurations entails unreasonably expensive computational costs. The authors applied the study to a large unidirectional axial flow fan unit for tunnel ventilation to operate in the forward direction under ambient conditions. This delivered cooling air to the tunnel under routine operation, or hot gases at 400°C under emergency conditions in the event of a tunnel fire. The simulations were carried out using the open source code OpenFOAM, within which they implemented a (very) large eddy simulation (VLES) based on one-equation SGS model to solve a transport equation for the modelled (sub-grid) turbulent kinetic energy. This sub-grid turbulence model improvement is a remedial strategy in VLES of high-Reynolds number industrial flows which are able to tackle the turbulence spectrum's well-known insufficient resolution. The VLES of the industrial fan permits to detect the unsteady topology of the rotor flow. This paper explores the main secondary flow phenomena's evolution and speculates on its influence on the actual load capability when operating at peak-pressure condition.

INTRODUCTION

The selection of the state-of-the-art industrial fan technologies for tunnel ventilation normally fulfills user demands that require high volume flow rates and total pressure rises. As such, the specified operating area falls in several cases within the range ordinarily characterizing mixed flow fans. In addition to these performance requirements, two additional factors contribute to the complexity of design processes of the fan range customized for emergency and routine operating modes [1, 2]. First, the fan must have installation in either a vertical or horizontal lay-out, and, second, the fan range must be able to accommodate the effect of unsteady pressure pulses which the trains generated in ventilation shafts [3-6].

These requirements imply levels of complexity in the design process and diversity in the operations that are significantly beyond the historic norm within the fan industry. Therefore, the application of

standard methodologies is inappropriate and significant changes are taking place in the design process of large industrial fans. Although the conventional approach to fan design has historically involved trial-and-error empirical methods that rely on the designer's experience of aerodynamics [7, 8], more recent approaches to the design of state-of-the-art fan units have utilised computational fluid dynamics (CFD) analyses at the early stage of the process. Amongst others, Vad [9] and Corsini *et al.* [10] have proposed improved designs. These scholars developed a family of high-performance swept fans for mine ventilation by feeding-back the three-dimensional (3D) design criterion with the computed secondary flow aerodynamics. Lee et al. [11] applied an inverse approach to the design of cooling fans for electronic appliances, which included the combined use of a 'design of experiments' step and CFD to explore the space available for design solutions. In doing so, the above mentioned scholars transferred design methodologies reliant on CFD to develop appropriate 3D blades [12].

Historically, aerodynamic considerations primarily have constrained large fan designers. Initially, they would produce an aerodynamic design by scaling smaller unit characteristics with the final design's actual performance which the experimental testing established. However, recent legislative developments and standards relating to tunnel ventilation system fans have impacted fan design, resulting in unusual design choices, e.g. increased tip gap or solidity and blade thickness which mechanical rather than aerodynamic implications drive.

It is apparent that the EN 12101-3 and ISO 21927-3 [3, 5] constraints on industrial fan designers are driving continuing market demand for fans that can provide higher performance and less noise. In responding to these constraints, industrial fan designers require a methodology that combines finite-element analysis (FEA) (for mechanical analysis) and CFD (for aerodynamic and aero-acoustic analysis) to provide a virtual prototyping design methodology that replaces traditional testing and evaluation methods in fan development. Although virtual-prototyping techniques are presently uncommon in the fan industry, they provide cross-functional evaluations of competing objectives and enable designers to consider 'downstream design issues' in the initial stages [13, 14]. The process of virtual prototyping reduces the need to build physical prototypes and facilitates the early identification of design problems, thus reducing product development costs. Sheard *et al.* [15] case study proposed virtual prototypes to characterize the aerodynamic and acoustic profiles of a new range of large industrial fans.

A key ingredient in building-up accurate virtual prototype is turbulence computations. U-RANS and hybrid LES/RANS turbulence closure usage allows the simulation only of (part of) the flow unsteadiness without fully accounting for the influence of turbulence spectrum on flow unsteadiness. The proper simulation of the unsteady aerodynamics is also crucial in providing physical insights of the secondary flow structure and in recognizing the major contribution to fan noise emission. On the other hand, proper LES solutions are hardly available in the open literature due to the formidable computational effort required to solve the turbulent spectrum up to the inertial sub-range (e.g. Schneider *et al.* [16]). However, in high Reynolds number turbomachinery flow VLES with a proper resolution of the larger turbulent scales in the computational domain [17] are inherently unable to solve turbulence scale up to the inertial sub-range. In such a condition, the hypothesis of stationary, isotropic vortex cascade does not hold because of the occurrence of localized backscattering phenomena. Consequently an appropriate sub-grid scale motion, able to take in account at least backscattering effect should be considered when VLES computations are performed (e.g. dynamic model of Germano or one-equation subgrid scale model of Davidson and Nielsen [18]).

In recent years, open source philosophy has provided a new impetus in CFD code development. An open source code allows researchers to collaborate in developing fluid-dynamic software with accurate numerical schemes, fast solution algorithms and a wide selection of flow models. In the present study the authors used the open source code OpenFOAM (www.openfoam.com) [19], already used to carry out Detached-Eddy-Simulation and LES of the industrial fan under scrutiny

[20, 21]. The use of U-RANS first order closure, hybrid LES/RANS and VLES is well established in turbomachinery and industrial flow predictions. Despite contradictory findings, the authors documented noticeable results for both steady and unsteady approaches [22-28].

In this paper, the authors discuss the unsteady aerodynamics of the industrial fan under scrutiny. After the illustration of the flow topology, the study accounts for the evolution of secondary flow phenomena in order to establish the link with the unsteady variation of fan load and losses.

DESCRIPTION OF THE FAN

The range of large industrial fans under scrutiny was designed to comply with the legislative framework embodied in the EN 12101-3 and ISO 21927-3 standards, in force for tunnel ventilation. According to the specifications, relating to the installed fan performance, large fans intended for application in tunnel and metro ventilation systems must operate at elevated temperatures during an emergency whilst meeting specified noise emission requirements (i.e. 80 dB(A) in emergency and 50 dB(A) during routine operations). In addition to these requirements for emergency and routine operating modes, the fan must run at different speeds and accommodate the effect of unsteady pressure pulses that trains generate in tunnels when they pass a ventilation shaft.

Table 1 lists the specifications of the fan range. It consisted of seven standard diameters, and the performance requirements span over a range of duties typical of tunnel ventilation systems.

Table 1 Fan range description

Size range, D_{tip}	1.4 m – 2.8 m
Performance standard	ISO 5801
Volume flow rate	10 m^3/s – 300 m^3/s
Total pressure rise	500 Pa – 3000 Pa
rpm	900, 1500
High temperature certification	200℃, 300℃ and 400℃

Specifically, the fan under investigation was a 2.24 m diameter uni-directional fan spun by a 4-pole motor at 1500 rpm [15]. Figure 1 shows the 2.24 m prototype fan, labeled 224 JFM, with newly designed blades suitable for one-time only emergency operation at 400°C. Table 2 specifies the geometrical data of the blade of 224 JFM fan.

Table 2 Fan blade data at midspan

Blade section	ARA-D	
Diameter at the tip (mm)	2240	
Blade count	16	
Hub-to-tip diameter ratio	0.5	
	Hub	*Tip*
Chord (mm)	143	92.5
Solidity (-)	0.64	0.21
Pitch angle (deg)	48	24

Moreover, Figure 2 describes the operating region of the ventilation fan under scrutiny in terms of pressure-volume characteristic curves when varying the pitch angle, as measured at the blade tip, from 8 deg to 24 deg.

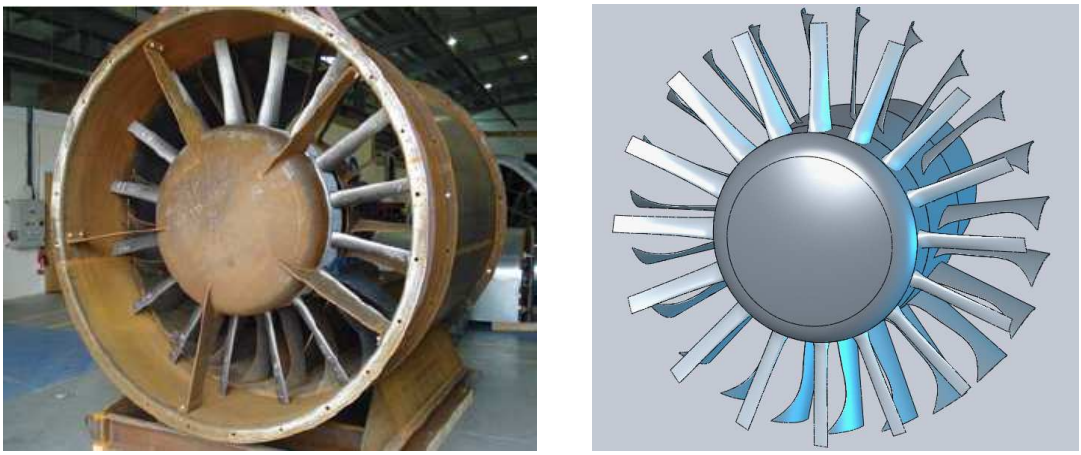

Figure 1: Fan 224JFM

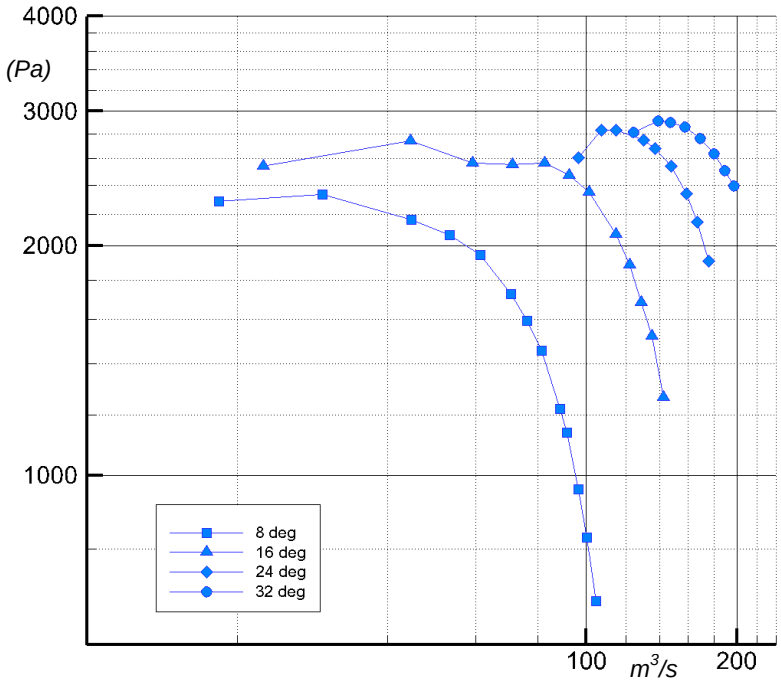

Figure 2: Total pressure-volume operating margin 224JFM

METHODOLOGY

Numerical technique

The computational analysis was based on the use of the open source finite volume CFD code OpenFOAM 1.7.x written in C++. The LES prediction of the fluid motion is computed by solving the filtered unsteady Navier-Stokes equations system. The sub-grid scales closure is modelled using the local dynamic k-equation model of Davidson and Nielsen [18], which the authors modified to take in account the occurrence of backscattering (i.e. kinetic energy transfer from smaller to greater scales), allowing the occurrence of negative sub-grid scale viscosity ν_{sgs}.

In the present computations the LES computation is based on a central difference space discretization with an accurate TVD scheme to prevent numerical instabilities and a second-order accurate implicit approach for time marching solution. Concerning the solution strategy, the discretised Navier-Stokes and turbulence equations are solved by adopting a ILU preconditioned

semi-iterative conjugate gradient linear solver, in combination with a PISO segregation scheme. To account for the fan rotation the original segregated solver (PISOFoam) was modified to consider the influence of Coriolis and centrifugal forces in the relative frame of reference.

The non-dimensional time step was set equal to 2×10^{-5} to keep the CFL number under the value of 0.7. Starting from a preliminary URANS computed flow field, the LES was performed for 2 flow through time (FTT) before acquiring flow field data. All the results in the next sections have been computed by collecting statistics during 1.5 FTT corresponding to 54 blade revolutions.

Numerical grid and boundary conditions

The authors conducted the test using a 24 deg pitch angle setting. The Reynolds number, based on tip diameter and rotor tip speed, is 8.7×10^6. In all the numerical campaigns normal air condition were assumed. The computational domain, which Figure 3 illustrates, extends half chord upstream of the leading edge and one chord downstream from the trailing edge.

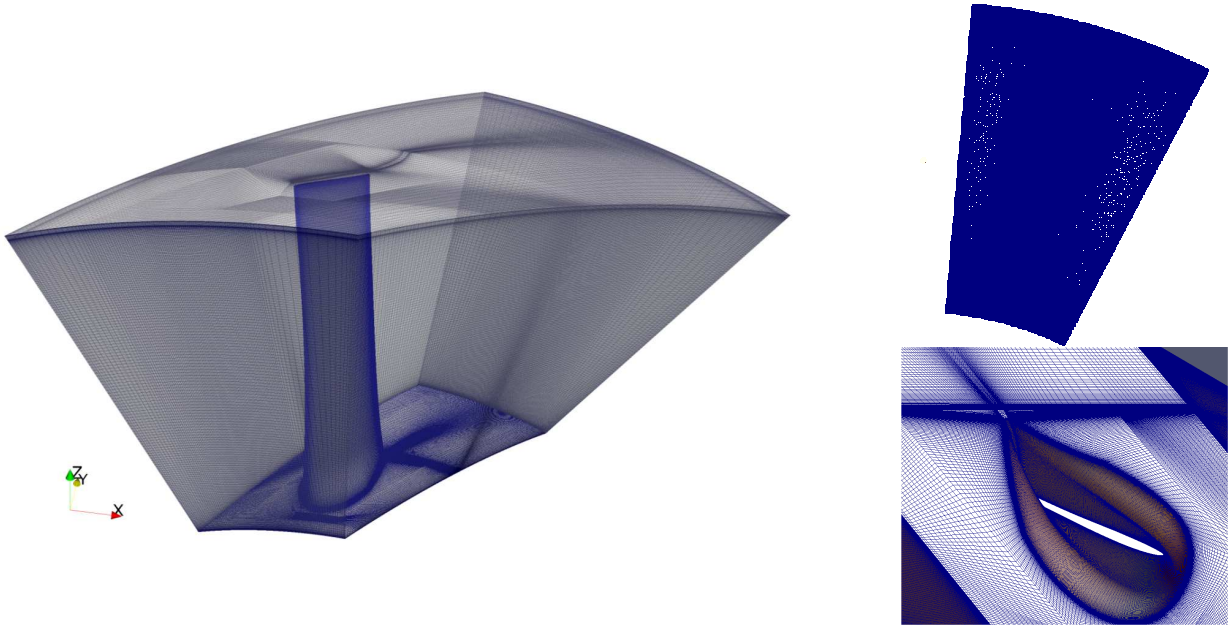

Figure 3: Computational domain and details of the grid

The mesh was built according to a non-orthogonal body fitted coordinate system with an immersed blade, using a block-structured topology. The mesh consisted of about 9×10^6 nodes and 8.8×10^6 hexahedral cells. Table 3 provides details of the rotor grid. Concerning the distribution of the elements in the axial direction, it consists of 16%, 50% and 34% of nodes respectively upstream of the leading edge, in the blade passage and downstream from it. Moreover, 55 cells are used to model the tip-clearance along the span. The mesh has an adequate clustering toward solid boundaries, with the ratio of minimum grid spacing on solid walls to mid-span blade chord set as 7×10^{-4} on the blade tip, casing wall and blade surfaces. The adopted grid refinement towards the solid surfaces controls the normalised wall distance y+ value about 1 on the first nodes row.

The inflow boundary conditions were set to account for the distortion effects induced by the spinner cone upstream the rotor leading edge [15]. Flow periodicity, upstream and downstream of the blade row, and Neumann outflow conditions complete the set of boundary data. Notably, whilst a steady velocity profile is imposed at the inlet, the flow unsteadiness develops within the rotor blading under the forcing influence of strong vortical structures generated on the endwalls.

Table 3 Fan mesh data

	Rotor
Nodes	9,021,968
Cells	8,862,550
Tip gap nodes	60,753
Tip gap cells	52,000
Blade surface cells	62,450
Averaged cell aspect ratio	1.34

RESULTS

The analysis of the unsteady aerodynamic of the fan is carried out with an angular setting of 24 deg in proximity of the peak-pressure operation close to the rotating stall incipience. In this condition, the fan delivers 120 m³/s with a total pressure rise of 2806 Pa. The investigation, first, focused on the reconstruction of the three-dimensional flow topology in the blade vane with emphasis on the secondary flow phenomena. Then, the authors speculated on the unsteady evolution of the load along the blade span when approaching the peak pressure limiting operation.

Flow topology

The authors discuss, first, the flow topology as per the evolution in time of the major vortical flow structures when the fan is operated close to its pressure limit. The vortex eduction analysis was, therefore, carried out by the prediction of the pressure Laplacian $\nabla^2 p$ iso-surfaces. This scalar quantity, which correlates to the well-known Q criterion, identifies coherent vortices in separated flows and was found to be more informative in case of flows bounded by compact walls [29].

The discussion of the flow topology is carried out using the method of Dubief & Delcayre [29] by plotting the evolution of instantaneous $\nabla^2 p$ iso-surfaces around the fan blade. Figure 4 shows a perspective view of the blade stacking at three instants with a constant time interval equivalent to 0,3 normalized time. In particular, Figure 4 illustrates the 3D view of the $\nabla^2 p$ =1000 iso-surfaces coloured by the relative velocity magnitude.

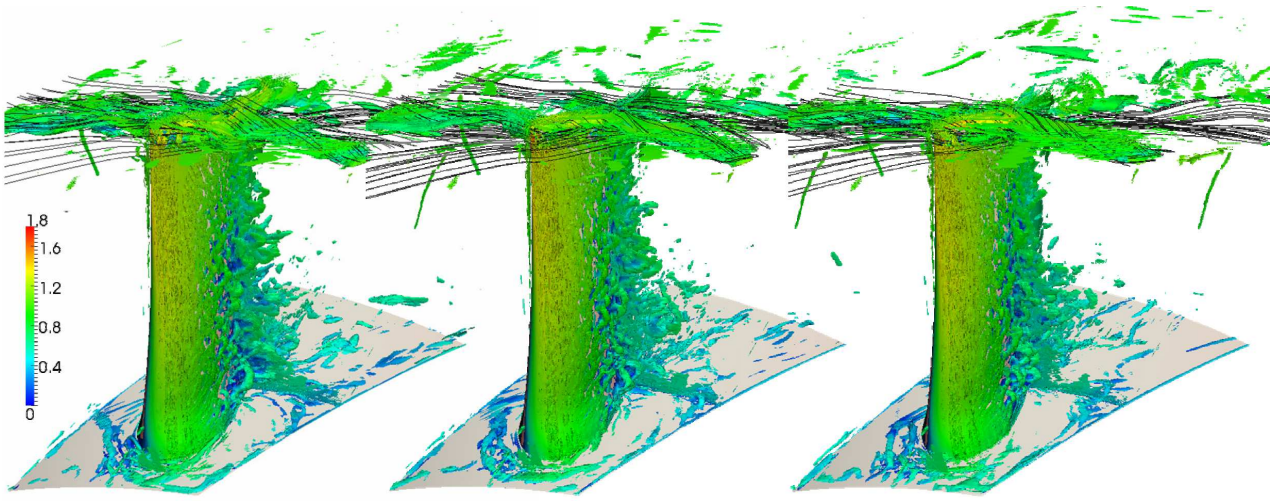

Figure 4: Flow topology $\nabla^2 p$ = 1000 iso-surfaces coloured with velocity magnitude.

As expected, vortical structures are generated though the lack of any unsteadiness at the inflow. The onset of vortical and secondary flow structures mostly correlated to the aerodynamic interaction

between the incoming flow and the blade which develops along the span with dramatic thickness variation as *per* the mechanical design requirements under the 400 °C specification.

On the hub the local bluntness of the blade resulted in a typical horse shoe vortex like structure whose suction and pressure side legs clearly marked the collateral boundary layer deviation about the leading edge. Moreover, the generation of a system of horseshoe vortices is evident including a smaller one close to the leading edge, and a second bigger one with a wider opening angle is present slightly upstream. As given by the time evolution in Figure 4, the horse-shoe vortex appeared to stably influence the inner endwall. Whilst the chordwise pressure field immediately strained the suction side leg, the pressure side one was found to have a longer streamwise evolution.

When looking at midspan, notably the shedding of vortical structures in the wake still develops under the influence of the aerodynamical design in the inner portion of the blade which was thickened due to structural reasons. This influence and the correlated intensity of the vortex shedding, gradually decreased when moving above midspan.

Finally, approaching the outer endwall, Figure 4 demonstrates that near the casing the tip leakage vortex represents the most relevant structure. Here, once again, the main tip leakage vortical formation moving across the blade vane at the leading edge developed stably while set of the tip leakage vortices, close to the blade surface, suffered an evident time dependence. Notably, the location of the larger tip leakage vortex was in accord with the actual operation in a pre-stall condition which is frequently correlated with a leakage vortex spillage.

In order to provide additional hints on the time evolution of those secondary phenomena found in the rotor flow topology, Figure 5 shows the contours of the helicity at the blade tip at three time abscissa again collected at constant time interval equivalent to 0,3 normalized time.

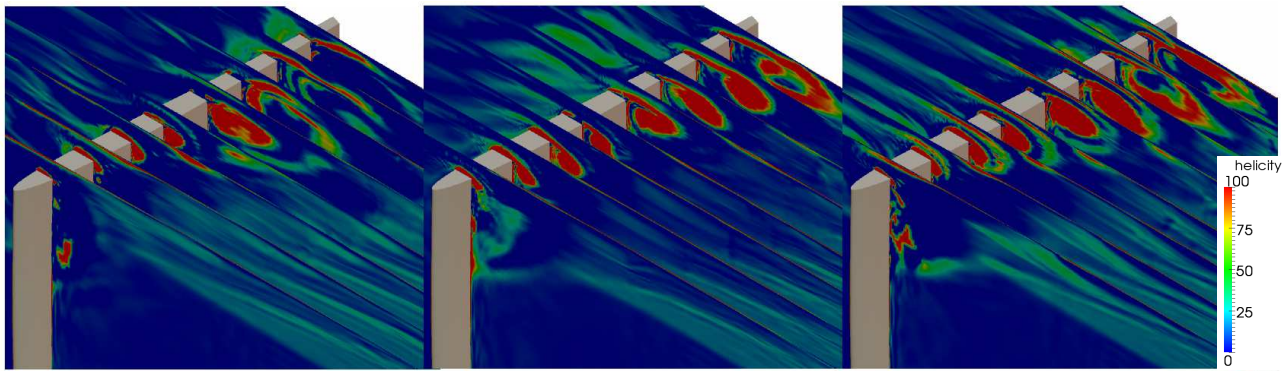

Figure 5: Tip leakage vortices eduction by the helicity contours.

Figure 5 gave a clear evidence of the multiple vortex behaviour which featured the fan under investigation according to the enlarged tip gap which resulted from the high temperature classification requirements. This geometrical element played a critical aerodynamic role and reflected in the large unsteadiness found in the time evolution of the swirling core at the blade tip. When comparing the helicity patterns, it was apparent that whilst the onset of the vortices stayed constantly in proximity of the blade leading edge, the swirling flow dynamics resulted in a periodical variation of the helicity level at the blade trailing edge.

To illustrate the evolution of the pressure side leg of the horse-shoe vortex at the hub, moreover, Figure 6 shows the contours of the enstrophy (which is defined as the integral of the square vorticity) at different axial section along the blade surface. The authors plotted the enstrophy contours on each section against the streamlines. Notably, when compared to the structures a the tip, the horse shoe vortex appeared to be stable. This circumstance is an indirect evidence of the origin of this peculiar vortical structure dictated by the geometry of the leading edge at the blade hub section.

Unsteady load analysis

A further step in the investigation was to quantify the influence of the aerodynamic unsteadiness on the work capability of the rotor. To this end, Figure 7 shows the distribution of the local diffusion factor (DF) computed according to the Lieblein definition [30].

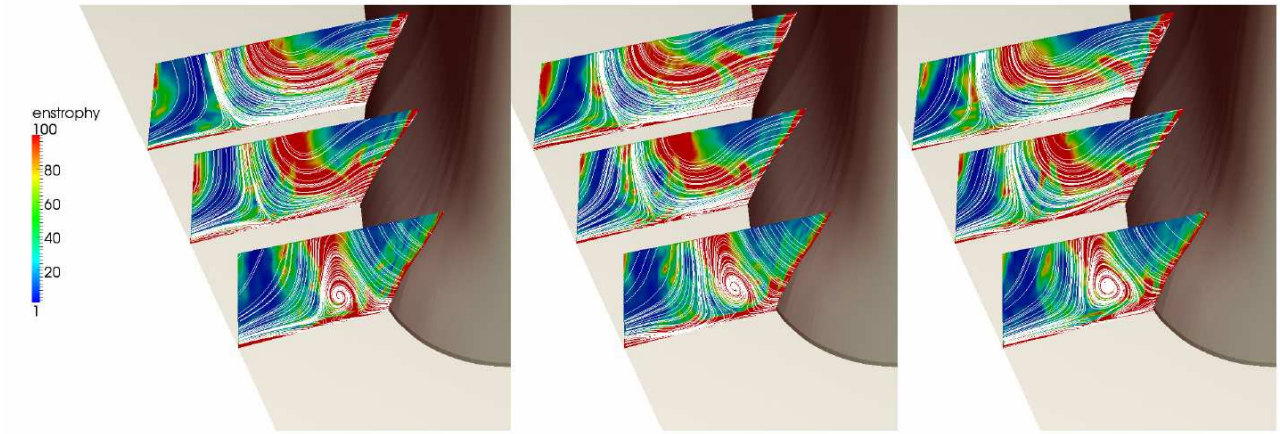

Figure 6: Horse-shoe vortex visualization by enstrophy contours and streamlines.

Figure 7 compares the evolution of DF behind the fan rotor by plotting the contours at three time abscissae taken at constant time interval 0,3 normalized time long.

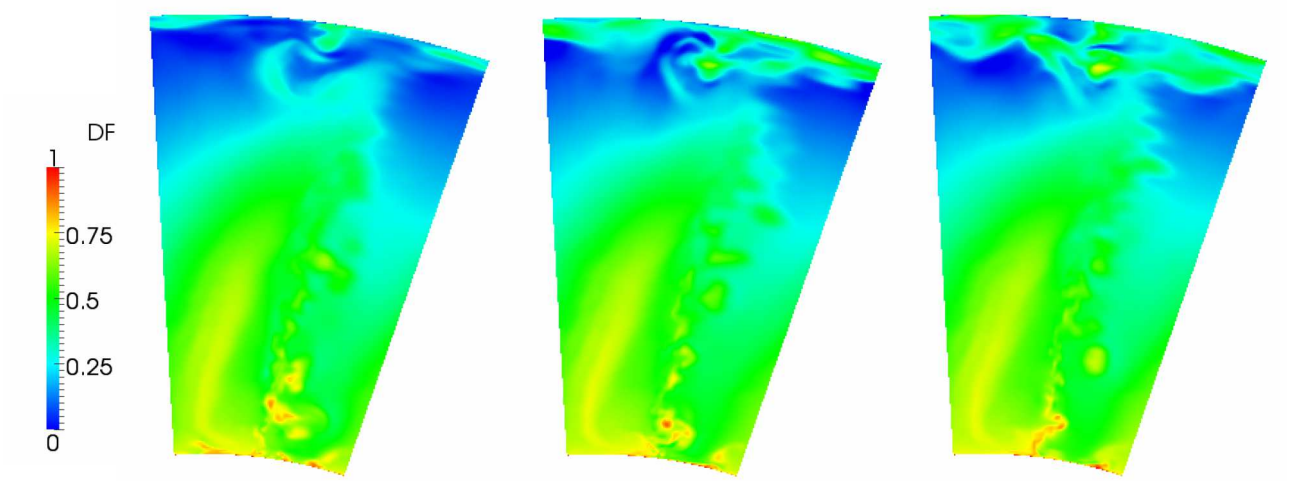

Figure 7: Diffusion factor DF evolution behind the rotor.

As expected the secondary flow structure affected the load condition along the blade span. In accordance with the flow topology findings, at the blade hub the deviation of the flow was influenced by the shedding of vortical structures. In particular, on the suction side the wake distorted steadily the DF distribution whilst on the pressure side of the blade it was possible to find a large unsteadiness as the result of the stronger horse-shoe vortex leg.

At the tip, where according to the prescribed radial work distribution the rotor is unloaded, the tip vortices produced large fluctuations in the local blade deviation and deceleration capability. Notably, this unsteady behaviour occurred at peak pressure condition with the rotor close to a pre-stall operation.

CONCLUSION

The authors carried out an analysis of the unsteady flow in a large industrial fan designed for one-time-only operation at 400 °C. The new design methodology, here under aerodynamic scrutiny, has facilitated development of a range of large fans that complies with the requirements of both EN 12101-3 and ISO 21927-3 during emergency operation.

The authors based their investigation on an Open Source solver, OpenFOAM, using an original very LES sensitized to the backscattering to give an interpretation of the detailed flow topology.

The study of the flow topology was conducted using a vortex eduction criterion based on the pressure Laplacian. The authors found that at the blade hub, a complex vortical pattern takes place as a consequence of the blade section's thickness distribution at the root which induces the formation of a horseshoe vortex system. On the other hand, the tip region features the presence of vortical structures that evolve and interact along the blade stacking line, being generated by the tip leakage vortex swirling core. The analysis of flow field demonstrated that, far from the endwall, the main source of unsteadiness is related to the wake development downstream from the trailing edge.

ACKNOLEDGMENTS

The authors wish to express their gratitude to *Fläkt Woods Ltd, Colchester UK*. Moreover, the authors are indebted to Mr Fabrizio Sciulli, Mr. Mario Fiorito and Dr. Giovanni Delibra who were instrumental in the fan design phase and in the numerical campaigns. We also thank MIUR for their generous support, and CASPUR for the computational resource made available on the Matrix cluster (HPC Grant 2010-288).

REFERENCES

[1] Lacroix, D., **1997**, – *New French Recommendations for Fire Ventilation in Road Tunnels*, Proc. 9th Int. Conf. on Aerodynamics & Ventilation of Vehicular Tunnels, Aosta Valley, Italy, pp. 103 – 123.

[2] Carvel, C., **1999**, – *The Effects of Ventilation on Fires in Tunnels*, Proc. Int. Tunnel Fire & Safety Conf., Rotterdam, The Netherlands.

[3] Sheard, A.G. & Jones, N.M., **2005**, – *Emergency Ventilation for Vehicular, Rail & Metro Tunnels*, Proc. Int. Congress: Safety Innovation Criteria Inside Tunnels, Dijon, Spain.

[4] Sheard, A.G. & Jones, N.M., **2006**, – *High Temperature Certification of Large Fans For Emergency Ventilation*, Proc. 12th Int. Symp. on Aerodynamics & Ventilation of Vehicle Tunnels, , Portoroz, Slovenia, pp 123-140.

[5] Sheard, A.G. & Jones N.M., **2008**, – *Approval of High-Temperature Emergency Tunnel-Ventilation Fans: The Impact of ISO 21927-3*, Proc. of ITA – AITES World Tunnel Congress and 34th General Assembly, Agra, India.

[6] ANSI/ASHRAE Standard 149-2000, *Laboratory Methods of Testing Fans Used to Exhaust Smoke in Smoke Management Systems*, Atlanta, **2000**.

[7] Wallis, R.A., **1961**, *Axial flow fans: design & practice*, George Newnes Ltd, UK.

[8] Daily, B.B., **1985**, *Woods practical guide to fan engineering*, Woods of Colchester Ltd, UK.

[9] Vad, J., **2001**, – *Incorporation of Forward Blade Sweep in the Non-Free Vortex Design Method of Axial Flow Turbomachinery Rotors*, Periodica Polytechnica, Mechanical Engineering Series, Vol 45-2, pp. 217-237.

[10] Corsini A., Rispoli F., Vad J., Bencze F., **2001**, – *Non free vortex flow effects in an axial flow rotor*, Periodica Polytechnica, Mechanical Engineering Series, Vol 45-2, pp. 201-216.

[11] Lee, K.Y., Choi, Y.S., Kim Y.L., Yun J.H., **2008**, – *Design of axial fan using inverse design method*, J. of Mech. Science & Tech., 22, pp. 1883-1888.

[12] Horlock, J.H., Denton, J.D, **2005**, – *A review of some early design practice using computational fluid dynamics & a current perspective*, ASME J. Turbomachinery, 127, pp. 5-13.

[13] Pratt, M.J., **1994**, – Virtual *prototypes & product models in mechanical engineering*, IFIP WG 5.10 on Virtual Environments & their Applications & Virtual Prototyping, pp. 113-128.

[14] Jasnoch, U., Kress, H., Rix, J., **1994**, *Towards a virtual prototyping environment*, IFIP WG 5.10 on Virtual Environments & their Applications & Virtual Prototyping, pp. 173-183.

[15] Sheard, A. G., Corsini, A., Minotti, S., Sciulli, F., **2009**, – *The role of computational methods in the development of an aero-acoustic design methodology: application to a family of large industrial fans*, CMMF'09, Sept 9-12, Budapest.

[16] Schneider , H., von Terzi, D., Bauer H.-J., **2010** – *Large-Eddy Simulations of trailing-edge cutback film cooling at low blowing ratio*, Int. J. Heat Fluid Flow, 31, Pages 767-77.

[17] Labois, M., Lakehal, D., **2011**, '*Very-Large Eddy Simulation (V-LES) of the flow across a tube bundle*' Nuclear Engineering & Design, 241, pp. 2075–2085.

[18] Davidson L., Nielsen P. **1996**, '*Large eddy simulations of the flow in a three-dimensional ventilated room*', 5th Int. Conf. on Air Distribution in Rooms, Yokohama, Japan, pp. 161-168.

[19] Jasak, H., **2010**, – *OpenFOAM: A year in review*, Fifth OpenFOAM Workshop, June 21-24, Gothenburg, Sweden.

[20] Borello., D., Corsini, A., Rispoli, F., Sheard, A.G., **2011**, – *DES of a Large Industrial Fan at Design Operation*, submitted to Journal of Power & Energy.

[21] Borello., D., Corsini, A., Rispoli, F., Sheard, A.G., **2012**, – *LES of the aerodynamics & aero-acoustic performance of an industrial fan designed for tunnel ventilation*, draft submitted to Turbo Expo 2012, ASME paper GT2012-69046.

[22] Corsini A., Rispoli F., **2005**, – *Flow analyses in a high-pressure axial ventilation fan with a non-linear eddy viscosity closure*, Int J Heat Fluid Fl, 17, pp. 108-155.

[23] Borello D., Hanjalic K., Rispoli F., **2005**, – *Prediction of turbulence & transition in turbomachinery flows using an innovative second moment closure modelling*, ASME Journal of Fluids Engineering, 127, pp.1059-1070.

[24] Borello D., Hanjalić K., Rispoli F., **2007**, – *Computation of tip-leakage flow in a linear compressor cascade with a second-moment turbulence closure*, Int. J. Heat Fluid Flow, 28, pp. 587-601.

[25] Borello, D., Delibra, G., Hanjalic, K., Rispoli, F. **2009**, – *Large-eddy simulations of tip leakage & secondary flows in an axial compressor cascade using a near-wall turbulence model*. Proc. IMechE Vol. 223 Part A: J. Power & Energy, pp. 645-655.

[26] Borello, D., Delibra, G., Hanjalić, K., Rispoli, F., **2010**, *Hybrid LES/RANS study of turbulent flow in a low speed linear compressor cascade with moving casing*, ASME paper GT2010-23755.

[27] Delibra G., Borello D., Hanjalić K., Rispoli F., **2009**, – *URANS of flow & endwall heat transfer in a pinned passage relevant to gas-turbine blade cooling*, Int. J. Heat Fluid Flow, 30, pp. 549-560.

[28] Delibra G., Borello D., Hanjalić K., Rispoli F., **2010**, – *A LES insight into convective mechanism of heat transfer in a wall-bounded pin matrix*, 14th Intern. Heat Transfer Conference, 2010, Washington DC, USA.

[29] Dubief, Y., Delcayre, F., **2000**, — *On coherent-vortex identification in turbulence*, J. of Turbulence, 1, 011.

[30] Lieblein, S, 1956, — *Experimental Flow in 2D Cascades, Ch VI of The Aerodynamic Design of the Axial Flow Compressor*, NACA RME 56B03, reprinted as NASA SP36, 1965.